Interfacially Compatibilized Poly(lactic acid) and Poly(lactic acid)/Polycaprolactone/Organoclay Nanocomposites with Improved Biodegradability and Barrier Properties: Effects of the Compatibilizer Structural Parameters and Feeding Route

S. Shafiei Sabet, A. A. Katbab

Faculty of Polymer Engineering, Amirkabir University of Technology, Tehran, Iran

Received 26 December 2007; accepted 30 July 2008
DOI 10.1002/app.29210
Published online 6 November 2008 in Wiley InterScience (www.interscience.wiley.com).

ABSTRACT: Nanocomposites with enhanced biodegradability and reduced oxygen permeability were fabricated via melt hybridization of organomodified clay and poly (lactic acid) (PLA) as well as a PLA/polycaprolactone (PCL) blend. The nanocomposite microstructure was engineered via interfacial compatibilization with maleated polypropylene (PP-*g*-MA). Effects of the compatibilizer structural parameters and feeding route on the dispersion state of the nanolayers and their partitioning between the PLA and PCL phases were evaluated with X-ray diffraction, transmission electron microscopy, and scanning electron microscopy. Although highly functionalized PP-*g*-MA with a low molecular weight was shown to be much more effective in the intercalation of PLA and the PLA/PCL blend into the clay gallery spaces, composite samples compatibilized by high-molecular-weight PP-*g*-MA with a lower degree of maleation exhibited lower oxygen permeability as well as a higher rate of biodegradation, which indicated the accelerating role of the dispersed nanolayers and their interfaces in the enzymatic degradation of PLA and PLA/PCL matrices. This evidenced a correlation between the nanocomposite structure and rate of biodegradation. The size of the PCL droplets in the PLA matrix was reduced by nanoclay incorporation, and this revealed that the nanolayers were preferentially wetted by PCL in the blend. However, PCL appeared as fine and elongated particles in the microstructure of the PLA/PCL/organoclay hybrids compatibilized by higher molecular weight and less functionalized PP-*g*-MA. All the PLA/organoclay and PLA/PCL/organoclay hybrids compatibilized with high-molecular-weight PP-*g*-MA displayed a higher dynamic melt viscosity with more pseudo solid-like melt rheological responses, and this indicated the formation of a strong network structure by the dispersed clay layers. J Appl Polym Sci 111: 1954–1963, 2009

Key words: barrier; biodegradable; blends; composites; organoclay

INTRODUCTION

Biopolymers are increasingly being studied to replace petroleum-based polymers.[1–4] The potential of these materials in medical devices, packaging, and automotive applications is being explored by many researchers and industries. Poly(lactic acid) (PLA), one of the most popular and important biodegradable polymers, is known as a linear aliphatic thermoplastic polyester with beneficial performances. This polymer exhibits acceptable physical properties, good processability on standard plastic equipment (extrusion, injection, and film and fiber formation), high biodegradability, and accessibility from renewable resources (biomass).[5,6] The last feature makes PLA friendly to the environment. Moreover, the properties of PLA can be modified in a controlled manner through changes in its stereochemical structure (in the polymerization stage, i.e., with a mixture of the L- or D-isomers) and through blending with selected polymers or filling with inorganic microparticles or nanoparticles.

Studies that have compared the performances of biopolymers and synthetic polymers in packaging applications[3,6] have shown that biodegradable polymers have high potential in packaging applications. However, there are some limitations to PLA usage in the packaging industry, which include low thermal stability, medium gas-barrier properties, and brittleness.[7] A feasible strategy to reduce the brittleness of PLA is blending with polycaprolactone (PCL).[8,9] PCL is a semicrystalline aliphatic polyester with a low tensile strength, high elongation at break (>400%), and a processing temperature similar to that of PLA. Therefore, it is expected to act as a plasticizing agent when blended with PLA. A potential

Correspondence to: A. A. Katbab (katbab@aut.ac.ir).

drawback of these blend systems is the increase in the gas permeability as a result of the poor gas-barrier properties of PCL.[10]

The preparation of nanocomposites has been considered a promising method to improve the gas-barrier properties[10–14] and biodegradability[12,13] of PLA and PLA/PCL blends. Few studies have used a compatibilizer to increase the degree of exfoliation of the layered silicates within the PLA matrix.[7,15,16] Paul et al.[7] showed that poly(ethylene glycol) is capable of plasticizing PLA and therefore increasing the chain mobility, and this can enhance the intercalation mechanism. Maleic anhydride as a polar monomer has also been used to modify nonpolar polymers to improve the exfoliation of layered silicates.[17,18] Petersson et al.[16] used PLA-*g*-MA as a compatibilizer to prepare exfoliated PLA/organoclay nanocomposites. However, the effects of interfacial compatibilizer structural parameters such as the molecular weight, melt viscosity, and functionality have not been extensively investigated in PLA/organoclay nanocomposite systems. The main goals of this work were to synthesize interfacially compatibilized nanocomposites based on PLA, PLA/PCL, and organomodified clay. Maleated polypropylene (PP-*g*-MA) was employed as a compatibilizer, and the microstructure was engineered by the variation of the molecular weight as well as the functionality of the compatibilizers. Correlations between the microstructure, biodegradation, and also barrier properties of the prepared nanocomposites were investigated.

EXPERIMENTAL

Materials

The PLA (4042D) used in this study was a commercial product of NatureWorks Co., Ltd. (Minnetonka, MN). This material had a density of 1.25 g/cm^3, a glass-transition temperature of 52°C, and a melting temperature of 135°C. Commercial-grade poly(ε-caprolactone) (PCL) was supplied by Solvay (Warrington, UK) under the trade name CAPA 6500 with a number-average molecular weight of 50,000 g/mol and a melting temperature of 58–60°C. The layered silicate used in this work was montmorillonite modified with methyl tallow bis-(2-hydroxyethyl) ammonium and was kindly supplied by Zhejiang FengHong Clay Co. (Hangzhou, China) with the commercial name of DK2. This organomodified clay had d_{001} basal spacings of 28.02 and 18.58 Å.

Two different PP-*g*-MAs were used as interfacial compatibilizers: Licocene with a maleic content of 7% and a melting point of 140°C was obtained from Clarient Co. (USA), and Polybond 3200 with a maleic content of 1% and a melting point of 163°C was obtained from Crompton Co. (Middlebury, CT).

Blend and nanocomposite preparation

Before the mixing process, PLA, PCL, and the organoclay were dried at 50°C *in vacuo* for 24 h to remove the remaining moisture. The blending of PLA and PCL and also compounding with the nanoclay were carried out in a HAAKE (Germany) Polylab internal mixer at 175°C and 80 rpm for 8 min. For the preparation of the master batch of Licocene (PP-*g*-MA with a low molecular weight) and organoclay (DK2), the blending temperature was kept at 155°C to achieve enough shear mixing and therefore a high degree of breakup of the clay tactoids.[18] The PLA/PCL blend composition was 80/20 (w/w).[8] The DK2 loading in all the prepared nanocomposites was 3 wt % with a compatibilizer-to-clay ratio of 3. The neat polymer was also processed under the same conditions to ensure that all samples received a comparable thermomechanical history.

Characterization

To evaluate the microstructure, wide-angle X-ray diffraction (WAXD) patterns were obtained by the use of a Phillips X'Pert X-ray diffractometer (Netherlands) with Cu Kα radiation ($\lambda = 1.54$ Å), an operating voltage of 40 kV, and a filament current of 40 mA at a scanning rate of 0.02° (2θ)/min. The patterns were recorded from 1.5 to 10° (2θ). Nanoscale structures of various nanocomposites were investigated by means of high-resolution transmission electron microscopy (TEM; EM 208, Philips Co.) operated at an accelerating voltage of 100 kV.

The morphology of PLA and PCL in the blend systems and their corresponding nanocomposites was examined with a Philips XL30 scanning electron microscope. For this purpose, the surfaces of the samples were previously coated by gold sputtering.

For further microstructural characterization, the melt viscoelasticity behavior of the PLA, PLA/PCL blend, and corresponding nanocomposites was studied with a Paar Physica UDS200 rheometric mechanical spectrometer (Austria) (parallel plate with a 25-mm diameter and 1-mm gap). All measurements were carried out at 175°C within the frequency range of 0.1–1000 s^{-1} and at the strain amplitude of 1%, which was found to be in the melt linear viscoelastic region of the samples.

The permeability of the prepared samples toward oxygen was measured according to ASTM 1434-82 with a GDP-C permeability tester. For this purpose, the samples were compression-molded into 300-μm-thick films with a hydraulic compression press at 185°C and then were immediately cold-quenched to prevent the formation of a crystalline structure in the obtained films and therefore remove the interference of crystallites with the barrier property.

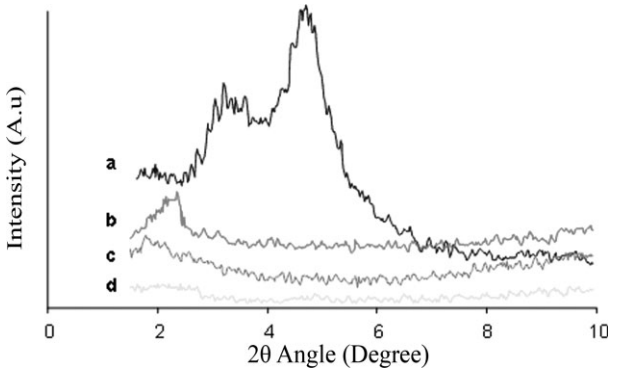

Figure 1 WAXD patterns of (a) pristine nanoclay DK2, (b) an uncompatibilized PLA/DK2 composite, (c) PLA/DK2 compatibilized with Licocene, and (d) PLA/DK2 compatibilized with Polybond 3200 (prepared by the direct melt-mixing process).

The biodegradability of the various samples was studied with a homemade composting instrument at $58 \pm 2^{\circ}C$.[19,20] The organic compost, with a C/N ratio of 6/1, was supplied by Biochemie Co. (Vienna, Austria). The test specimens were prepared by compression molding at 180°C in the shape of a sheet with dimensions of $3 \times 3 \times 0.1$ cm^3 and were quickly quenched.

RESULTS AND DISCUSSION

Nanocomposite structure

The degree of intercalation/exfoliation of the organoclay particles dispersed in a polymer matrix is reflected in the X-ray diffraction (XRD) spectrum of the nanocomposites. The shift of the characteristic diffraction peaks of the clay to the lower angles indicates an increase in the d_{001} basal spacing of the clay nanolayers, whereas the disappearance of the diffraction peaks reflects exfoliation of the clay platelets. Broadening of the peaks suggests partial exfoliation.[19]

Figures 1 and 2 present the results of the XRD analysis of the neat DK2 powder and corresponding uncompatibilized and compatibilized PLA/DK2 and PLA/PCL/DK2 nanocomposites within the range of $2\theta = 1$–10°.

It can be clearly seen in these figures that neither of the two characteristic diffraction peaks of DK2 appears in the XRD patterns of the composites, and this indicates possible exfoliation of the clay platelets. However, a broadened low-intensity peak appearing at a low diffraction angle in the spectrum of the PLA/DK2 and PLA/PCL/DK2 composites suggests the existence of some disordered intercalated clay stacks. The broadening of this peak could be explained by the partial disruption of parallel clay stacks swollen by the PLA or PCL chains. Therefore, the coexistence of exfoliated and intercalated clay stacks is observed for all these composite samples. Moreover, the intensity of this peak is less pronounced in the spectrum of the compatibilized composites, and this supports the enhanced interfacial interaction between the clay platelets and PLA or PCL molecules.

XRD patterns of interfacially compatibilized PLA/DK2 and PLA/PCL/DK2 composites prepared by direct and master-batch incorporation of Licocene and Polybond 3200 as compatibilizers are illustrated and compared in Figures 3 and 4, respectively.

According to Figure 3, the inclusion of Licocene and Polybond 3200 compatibilizers in the form of a master batch in the PLA matrix (L-m and P-m) led to a decrease in the ordered clay structure, which can be explained by the enhanced interaction of PLA chains with the DK2 silicate layers by the compatibilizer molecules. In the case of PLA/PCL/DK2 composites prepared with the Licocene master batch (Fig. 4; L′-m), there is no diffraction peak between 1 and 10°, and this indicates a high level of clay nanolayer exfoliation throughout the PLA/PCL matrix. The enhancement in the separation and exfoliation of the DK2 clay platelets can also be observed for the PLA/PCL/DK2 composites interfacially compatibilized by Polybond 3200 via master-batch incorporation of Polybond 3200/DK2 into the PLA/PCL blend system (Fig. 4; P′-m). On the basis of these results, we are led to the conclusion that master-batch melt mixing of the compatibilizers and DK2 organoclay with PLA or PLA/PCL is much more effective in achieving a high degree of clay exfoliation into the matrix.

Although the interlayer spacing between the neat clay nanolayers in their original form and in the microstructure of the nanocomposites can be

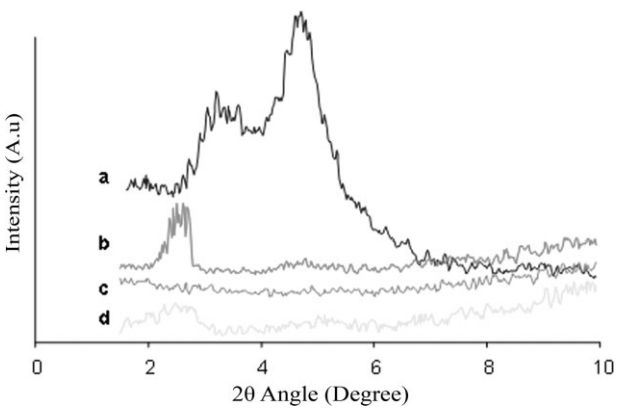

Figure 2 WAXD patterns of (a) pristine nanoclay DK2, (b) an uncompatibilized PLA/PCL (80/20)/DK2 composite, (c) a PLA/PCL (80/20)/DK2 composite compatibilized with Licocene, and (d) a PLA/PCL (80/20)/DK2 composite compatibilized with Polybond 3200 (prepared by the direct melt-mixing process).

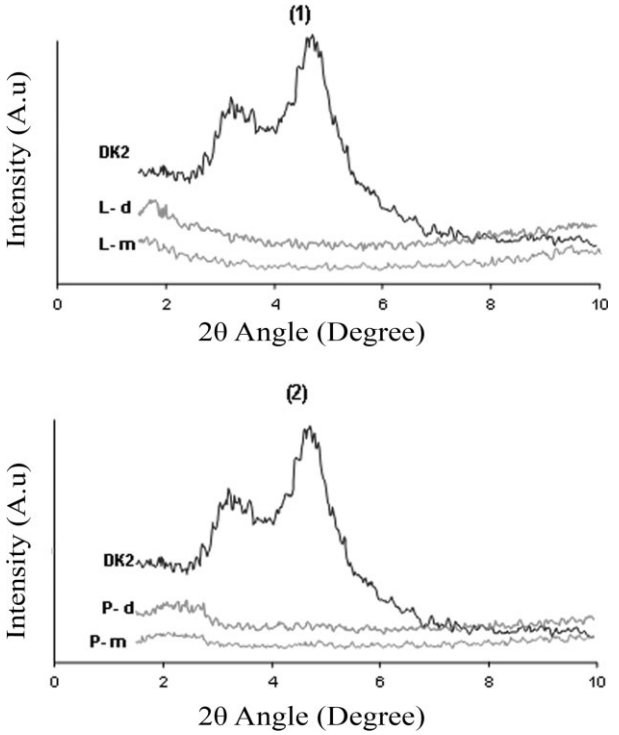

Figure 3 WAXD patterns of pristine nanoclay DK2 and (1) PLA/DK2/licocene and (2) PLA/DK2/Polybond 3200 prepared by direct (d) and master-batch (m) incorporation of the compatibilizers.

determined with the WAXD method, nevertheless, little can be said about the spatial distribution of the nanolayers or any structural inhomogeneities in the nanocomposites. As some layered silicates initially do not exhibit a well-defined basal reflection, peak broadening and intensity decreases are difficult to study systematically. Therefore, the developed microstructure in the polymer nanocomposites cannot be discussed solely on the basis of WAXD, and it needs to be analyzed by visual methods such as TEM. Figures 5 and 6 present TEM micrographs of different PLA/clay and PLA/PCL/clay nanocomposites, respectively. Nanometric-range intercalated and/or exfoliated clay tactoids can be clearly seen in these figures. Dark lines correspond to the cross section of the clay sheets, and the bright area between two adjacent lines is the interlayer spacing or gallery. Figure 5(a) presents the TEM image of an uncompatibilized PLA/DK2 composite sample. DK2 tactoids as stacks with different thicknesses as well as thin nanolayers are present in the microstructure of this composite. In other words, partial delamination or separation occurred in the absence of a compatibilizer, and this is in accordance with the diffraction peak appearing in the XRD patterns of this sample [Fig. 1(b)], suggesting the presence of periodicity. The incorporation of Licocene or Polybond 3200 as a compatibilizer led to more intercalation and separation of nanolayers and therefore their better dispersion in the PLA matrix, and this is consistent with the decrease in the XRD peak intensity shown in the XRD patterns [Fig. 1(c,d)]. However, the TEM micrograph of the PLA/DK2 nanocomposite prepared in the presence of Polybond 3200 as a compatibilizer reveals longer nanolayers with more orientation versus those composed of the Licocene compatibilizer. This can be explained by the higher melt viscosity of the Polybond 3200 compatibilizer, which exerts greater stress on the clay tactoids during the mixing process, leading to more separation of the intercalated clay nanolayers and their better dispersion and therefore an increase in the proximity of the platelets. This results in an increasing degree of flocculation via interlayer interactions. The enhanced breakdown of the clay tactoids as a result of the increased shear melt viscosity by the incorporation of high-molecular-weight compatibilizers into the PP/clay nanocomposite systems has also been reported by others.[18] The higher melt viscosity of the nanocomposite with Polybond 3200 as a compatibilizer is suggested as a cause of more orientation of the clay platelets during the compression-molding process.

TEM micrographs of the uncompatibilized and compatibilized PLA/PCL/DK2 composites are also illustrated in Figure 6. The TEM image of

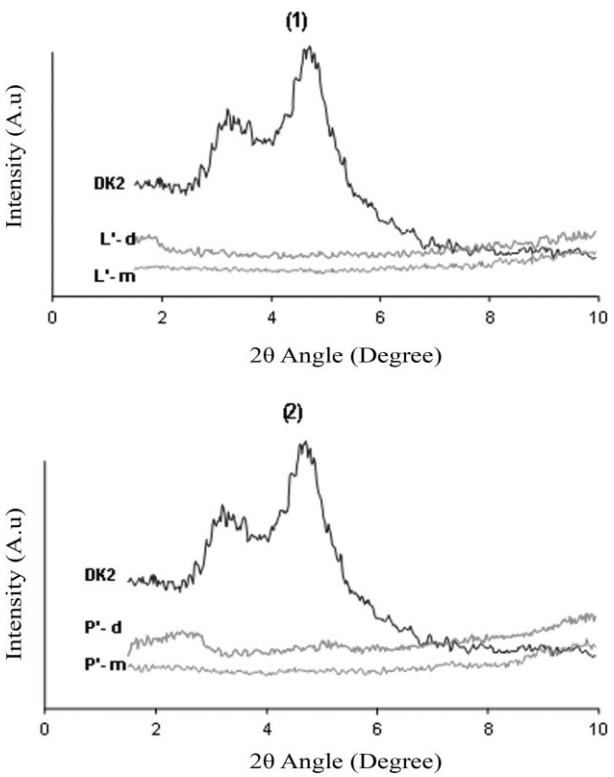

Figure 4 WAXD patterns of (1) PLA/PCL (80/20)/DK2/licocene and (2) PLA/PCL (80/20)/DK2/Polybond prepared by direct (d) and master-batch (m) feeding routes.

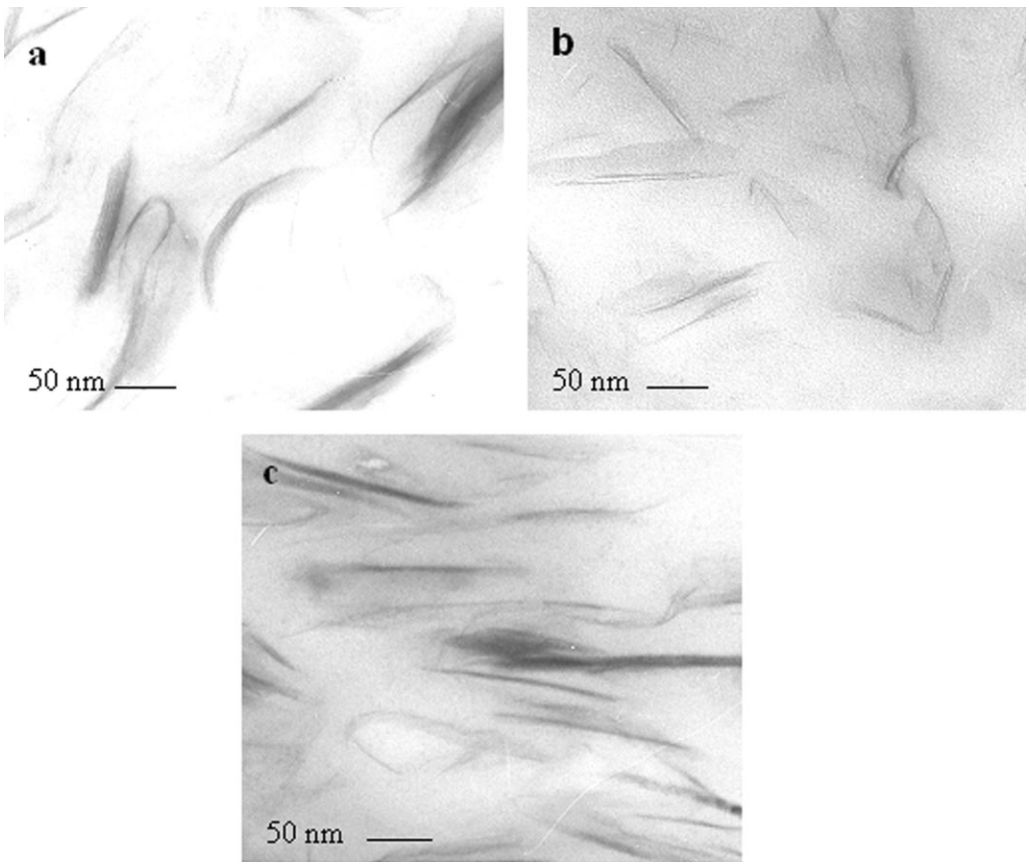

Figure 5 Bright-field TEM images of (a) an uncompatibilized PLA/DK2 nanocomposite, (b) a PLA/DK2 nanocomposite interfacially compatibilized with Licocene, and (c) a PLA/DK2 nanocomposite interfacially compatibilized with Polybond 3200 (prepared by the direct melt-mixing process).

uncompatibilized PLA/PCL/DK2 [Fig. 6(a)] shows a finer and more uniform distribution of clay platelets in the PLA/PCL matrix in comparison with the uncompatibilized PLA/DK2 composite [Fig. 5(a)], and this is consistent with the higher diffraction peak intensity appearing in the XRD pattern of the uncompatibilized PLA/PCL/DK2, as shown in Figure 2(b). This might be attributed to the higher polarity of the PLA/PCL matrix versus that of neat PLA and hence more affinity of the PLA/PCL blend for intercalation into the clay gallery spaces. Moreover, as can be seen in Figure 6(c), longer clay platelets with a more planar alignment appear in the TEM image of the PLA/PCL/DK2 nanocomposite composed of Polybond 3200. This indicates again a higher degree of exfoliation of the clay platelets and therefore their possible flocculation, as explained in the case of the PLA/DK2/Polybond 3200 system.

To further study the effects of the compatibilizer structural parameters on the prepared nanocomposite microstructure, scanning electron microscopy (SEM) was also performed on the gold-coated fractured surfaces of the samples, as illustrated in Figure 7.

Figure 7(a) presents the SEM micrograph of an unfilled simple blend of PLA/PCL (80/20 w/w). It can be clearly seen that PCL appears in the form of a semicontinuous phase with dispersed and interconnected large droplets, and this indicates the immiscibility of those two phases. However, the incorporation of the nanoclay particles into the PLA/PCL blend led to the reduction of the size of the PCL droplets dispersed in the PLA matrix, and this suggests that the clay platelets, which carry negative surface charges, behave as barriers for the coalescence of the PCL droplets because of the existence of repulsive forces between the nanoplatelets. The addition of Licocene resulted in the size of the PCL dispersed phase increasing, whereas in the case of the sample composed of Polybond 3200, a uniform dispersion of the PCL droplets with a reduced size can be observed. This could be the result of the lower melt viscosity of Licocene, which can act as a plasticizer, leading to fewer shear breakdowns of the PCL droplets during the melt-mixing process.

Melt rheology

To better understand the extent of the interfacial interaction between the clay nanolayers and PLA or PLA/PCL matrices and also the developed

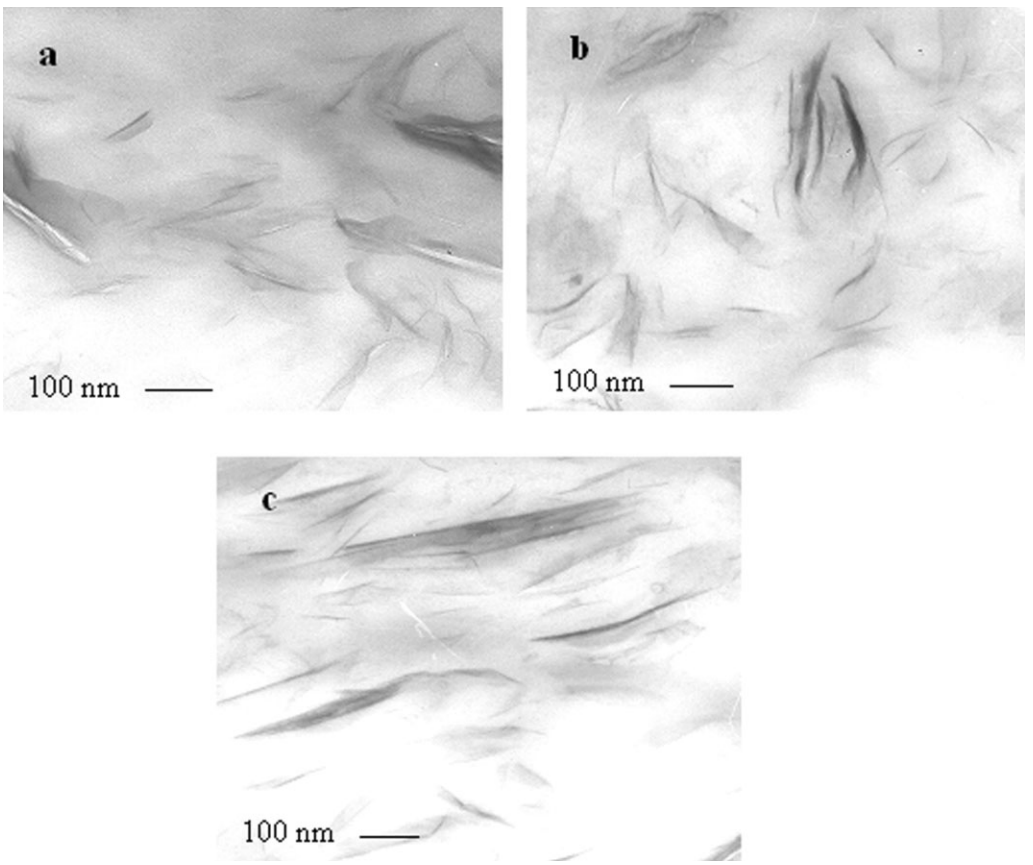

Figure 6 Bright-field TEM images of (a) an uncompatibilized PLA/PCL/DK2 nanocomposite, (b) a PLA/PCL/DK2 nanocomposite interfacially compatibilized with Licocene, and (c) a PLA/PCL/DK2 nanocomposite interfacially compatibilized with Polybond 3200 (prepared by the direct melt-mixing process).

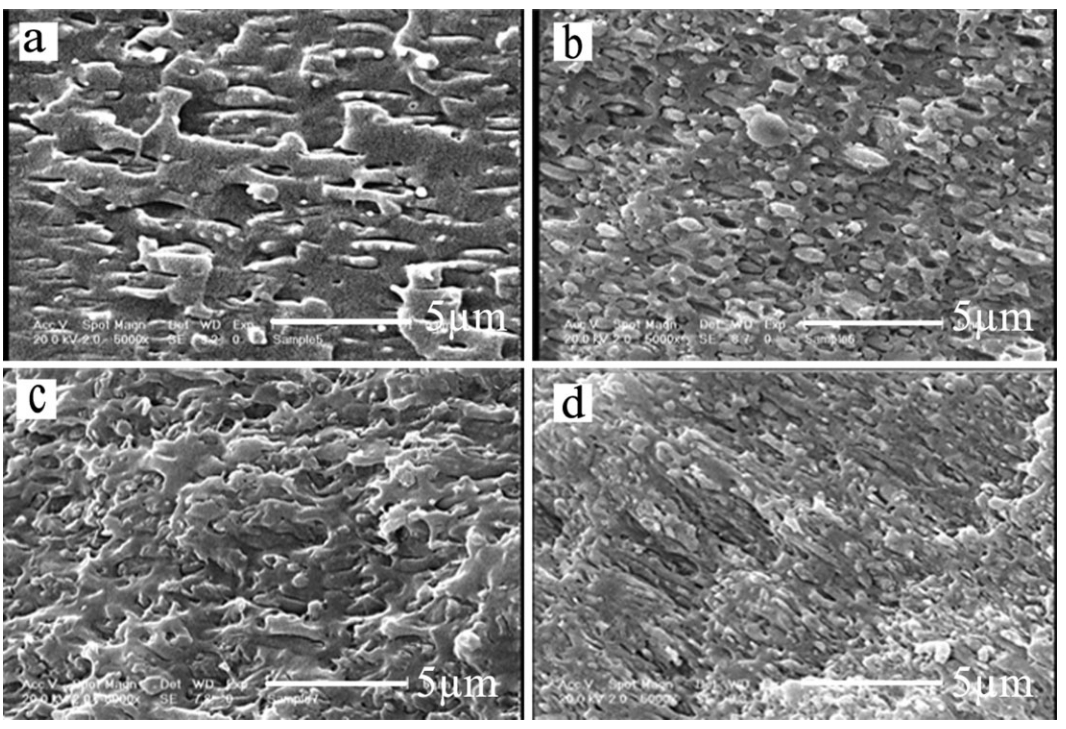

Figure 7 SEM micrographs of cryofractured surfaces of (a) PLA/PCL (80/20), (b) PLA/PCL (80/20)/DK2, (c) PLA/PCL (80/20)/DK2/Licocene, and (d) PLA/PCL (80/20)/DK2/Polybond 3200.

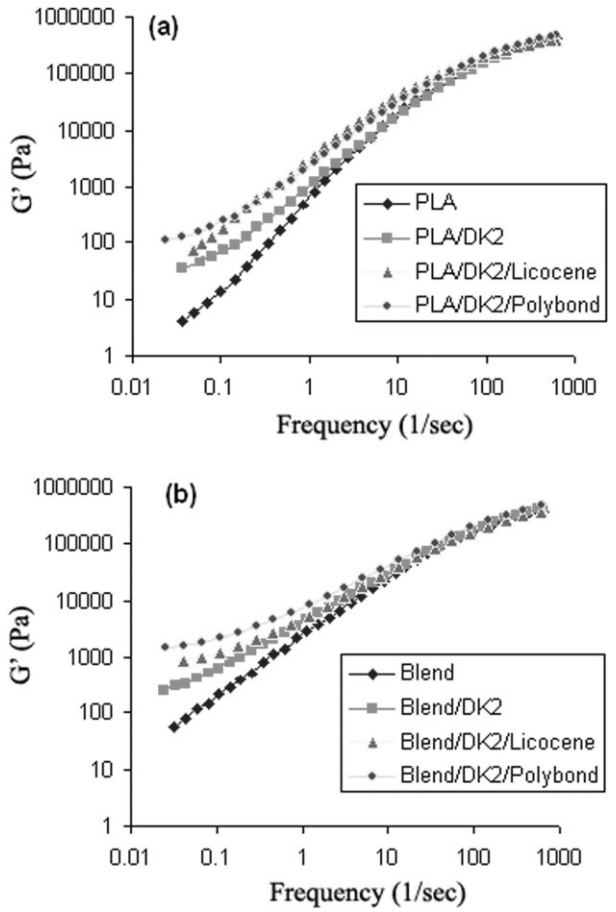

Figure 8 Frequency dependence of the melt dynamic storage modulus (G') of (a) PLA and PLA/clay nanocomposites and (b) the PLA/PCL (80/20) blend as the matrix and its corresponding nanocomposites.

microstructure, the melt viscoelasticity behavior of the composite samples was also evaluated. For this purpose, the melt dynamic linear viscoelastic region of the various samples at a strain of 1% was first determined by a dynamic strain sweep. The storage modulus, loss modulus, and complex viscosity obtained from the dynamic frequency scan measurements for the pristine PLA, PLA/PCL (80/20) blend, and corresponding nanocomposites are presented in Figures 8–10. At high frequencies (frequency $>$ 10/s), the viscoelastic behavior of all the nanocomposites is the same. On the other hand, at low frequencies (frequency $<$ 10/s), the enhancement of the storage modulus of the nanocomposites over their pristine counterparts is prominent. In addition, nonterminal and pseudo-solid-like behavior is also evidenced for the interfacially compatibilized PLA and PLA/PCL nanocomposites, especially for those based on Polybond 3200. It can be clearly seen that all the nanocomposites composed of Polybond 3200 exhibit more pseudo-solid-like behavior within a low-frequency region, and this indicates the formation of stronger percolated networks by the dispersed clay nanoplatelets.[21–27]

As can be seen in Figures 8–10, the addition of an interfacial compatibilizer and its structural parameters can play important roles in the development of the microstructure and melt viscosity of PLA/clay and PLA/PCL/clay nanocomposites. In Figure 10, it can be observed that all the molten interfacially compatibilized PLA and PLA/PCL nanocomposites exhibit a greater tendency for shear thinning than both uncompatibilized nanocomposites as well as the pristine polymer matrices, and this indicates the formation of network structures by the intercalated and exfoliated clay nanolayers dispersed throughout the compatibilized nanocomposites.[28]

Effects of the feeding route of the compatibilizer on the viscoelastic behavior of PLA/clay nanocomposites are illustrated in Figure 11. It can be observed that the incorporation of the compatibilizer in the form of a master batch led to more nonterminal and solid-like behavior within the low-frequency

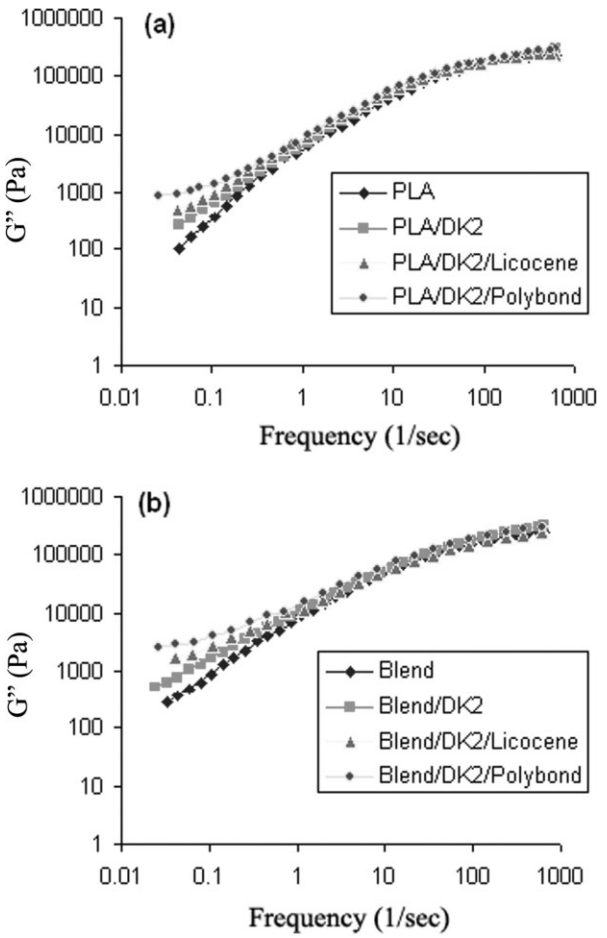

Figure 9 Frequency dependence of the dynamic loss modulus (G'') of (a) PLA and PLA/clay nanocomposites and (b) the PLA/PCL (80/20) blend as the matrix and its corresponding nanocomposites.

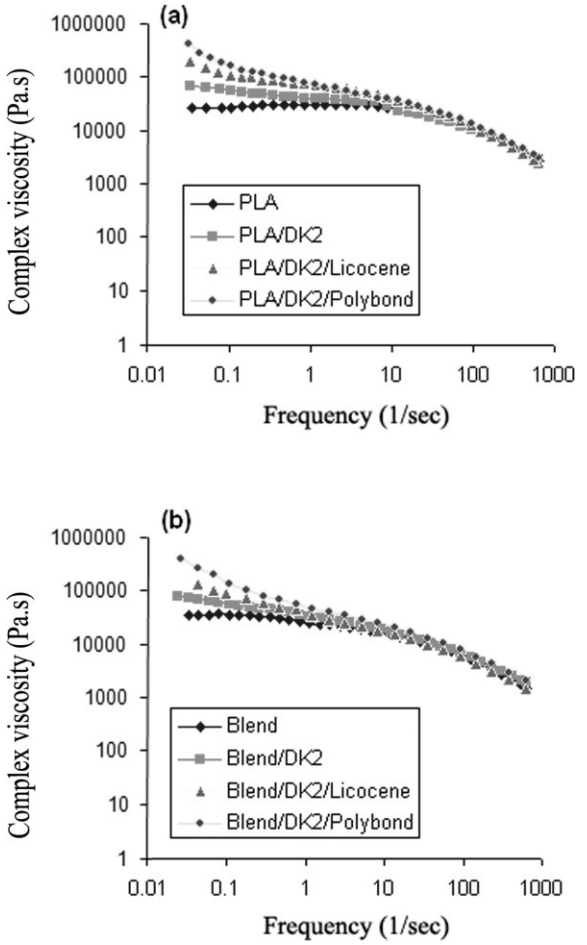

Figure 10 Complex viscosity versus the frequency for (a) the PLA matrix and its nanocomposites and (b) the PLA/PCL (80/20) blend and its corresponding nanocomposites.

region. This is consistent with the XRD patterns exhibited in Figure 3.

O_2 gas permeability

Layered structure nanofillers such as nanoclay are believed to be able to reduce the gas permeability of polymer matrices by the formation of a tortuous path by the filler nanolayers, which retard the diffusion and passage of the gas molecules through the matrix.[11–14,29]

However, gas-barrier properties of nanocomposites based on layered silicates are primarily governed by a few factors, including the filler volume fraction, dispersed silicate layer aspect ratio, and extent of dispersion of silicate layers as well as their orientation in the polymer matrix. The O_2 gas permeability coefficients of the pure PLA and PLA/PCL blend as well as their corresponding prepared nanocomposites with DK2 nanoclay are presented in Table I. It is obvious from this table that the inclusion of PCL in the PLA matrix resulted in increasing O_2 permeability, which can be attributed to the higher oxygen permeability of PCL versus that of PLA.[10] The incorporation of DK2 nanoclay into the PLA and PLA/PCL led to the decrease in the O_2 permeability. The PLA/DK2 and PLA/PCL/DK2 nanocomposites interfacially compatibilized by Polybond 3200 exhibited lower oxygen permeability, and this is consistent with their corresponding microstructures presented in Figures 5(c) and 6(c). Longer and flocculated dispersed silicate layers enlarged the diffusing path, and this resulted in an improved barrier property of the nanocomposites based on Polybond 3200 as an interfacial compatibilizer. Although the inclusion of Licocene enhanced the separation of clay nanolayers, the higher permeability coefficient exhibited by the nanocomposites based on Licocene versus those of the corresponding uncompatibilized and compatibilized ones with Polybond 3200 can be explained by the lubricating effect of low-molecular-weight Licocene in the melt state, which can retard the packing of the PLA and PCL chains during the quenching process.

Biodegradability

The most interesting result is the enhanced biodegradability of the PLA and PLA/PCL (80/20) blend loaded with nanoclay. One of the problems associated with PLA and its blends with PCL is the slow rate of biodegradation versus the rate of waste accumulation. In this work, the biodegradation of all the samples was studied in a compost environment at 58 $\pm$ 2°C, as the rate of degradation of pure PLA is very slow at the ambient temperature.[4,30] The residual weight percentages of the initial test samples with time (weight loss), which reflect the structural changes in the test samples, are given in Figure 12. It is obvious that the PLA and PLA/PCL nanocomposites are more sensitive toward biodegradation than the neat polymer matrices. This shows the catalytic role of the clay interfaces in the hydrolytic degradation of PLA and PCL chains. However, all the PLA/PCL/clay nanocomposites show a longer induction time and a lower rate of biodegradation in comparison with their counterpart PLA/clay nanocomposites. This can be attributed to the lower rate of biodegradation of PCL phases dispersed throughout the PLA matrix.[31] Therefore, it is concluded that blending PLA with PCL weakens the oxygen gas-barrier property as well as the rate of biodegradation, although mechanical properties are optimized.[9,32–34] The compost degradation of a biodegradable polymer occurs by a two-step process. During the initial phases of degradation, the high-molecular-weight matrix chains hydrolyze into lower molecular weight oligomers. This reaction can be accelerated by both temperature and moisture. Fragmentation of the plastic occurs during this step.

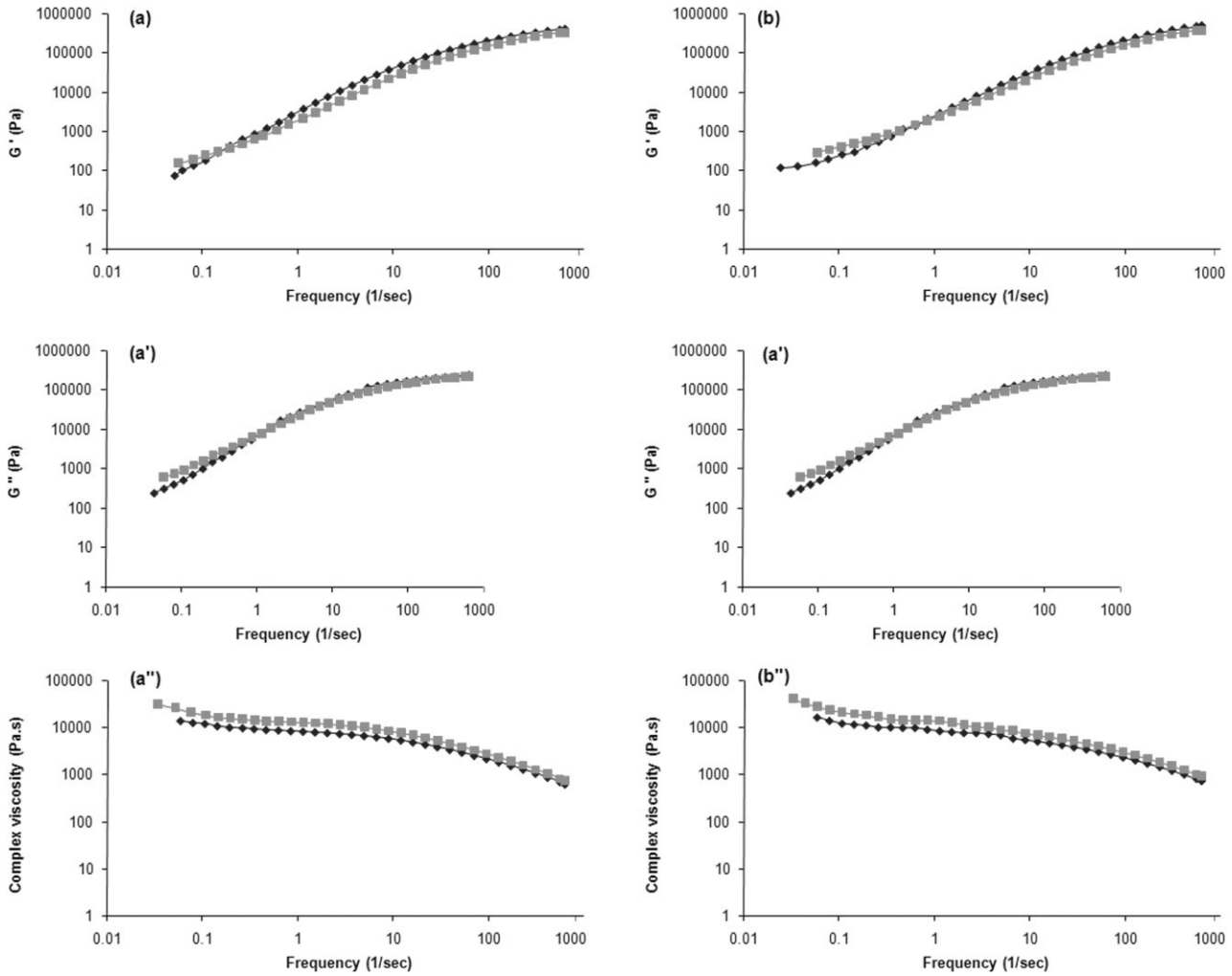

Figure 11 Frequency dependence of the dynamic storage modulus (G'), loss modulus (G''), and complex viscosity of interfacially compatibilized PLA/clay nanocomposites with (a,a′,a″) Licocene and (b,b′,b″) Polybond 3200 prepared by both (◆) direct and (■) master-batch methods.

Then, microorganisms in the compost environment continue the degradation process by converting these lower molecular weight components into CO_2, water, and humus.[4,30] Therefore, any factor that increases the hydrolysis tendency of the matrix ultimately controls the rate of degradation. It is thought that the presence of terminal hydroxylated edge groups of the DK2 nanolayers is responsible for the accelerated biodegradation of PLA and its blends. These hydroxyl groups start heterogeneous hydrolysis of the matrix after absorbing water from the compost, and because of this type of hydrolysis, the matrix becomes very small fragments and disappears with the compost.[19,20] In the case of samples containing PP-*g*-MA as a compatibilizer, because of better dispersion of the silicate layers and thus more available hydrolyzable sites, this effect is more significant.

TABLE I
Oxygen Permeability Coefficients of the Pure PLA, PLA/PCL Blend, and Their Corresponding Nanocomposites

Sample	Permeation (cm^3/m^2 d bar)	Relative permeability coefficient[a]
PLA	24.8	1.000
PLA/DK2	20.2	0.814
PLA/DK2/Licocene	22.5	0.907
PLA/DK2/Polybond 3200	18.4	0.742
Blend	43.2	1.000
Blend/DK2	39.3	0.909
Blend/DK2/Licocene	40.1	0.928
Blend/DK2/Polybond 3200	34.2	0.791

[a] Composite permeability coefficient/matrix permeability coefficient.

CONCLUSIONS

Interfacially compatibilized nanocomposites based on PLA, PLA/PCL, and DK2 organoclay with

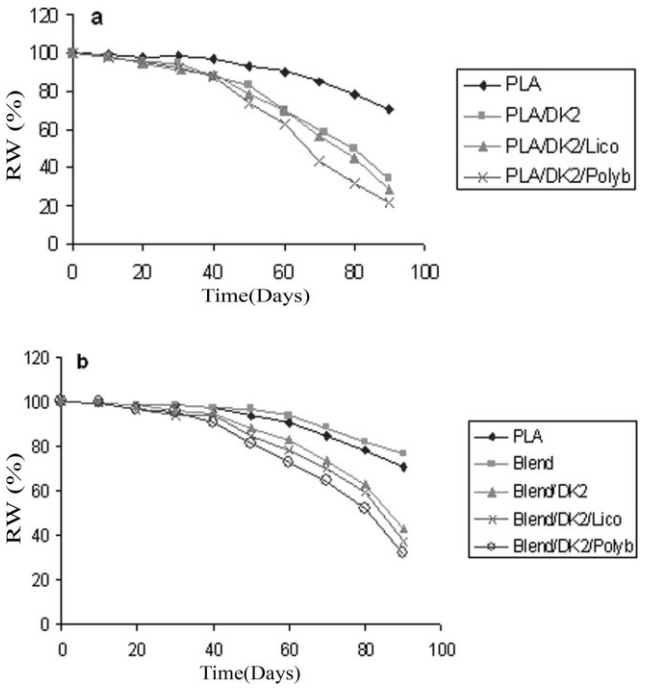

Figure 12 Time dependence of the residual weight (RW) of (a) PLA and its corresponding nanocomposites and (b) the PLA/PCL (80/20) blend and its associated nanocomposites.

enhanced barrier properties and enzymatic degradation were prepared. The degree of biodegradability was found to be controlled by the clay dispersion state and therefore the extent of interfacial interaction between the polymer matrix and nanolayers. All interfacially compatibilized nanocomposites exhibited enhanced biodegradability over the uncompatibilized counterparts. PLA and PLA/PCL nanocomposites based on DK2 nanoclay and a high-molecular-weight compatibilizer (Polybond 3200) exhibited more improved barrier properties toward oxygen molecules and also enhanced biodegradability versus those based on a low-molecular-weight compatibilizer (Licocene). This was consistent with the presence of longer silicate layers with their better dispersion in the microstructure of the nanocomposites compatibilized by Polybond 3200. This evidenced the accelerating role of the silicate platelets and their interfaces in the biodegradability of PLA and PLA/PCL blends. However, the incorporation of the compatibilizers in the form of a master batch into the polymer/clay mixture during the mixing process was found to be effective in increasing the degree of exfoliation of the silicate layers.

References

1. Vert, M.; Schwarch, G.; Coudane, J. J Macromol Sci Pure Appl Chem 1995, 32, 787.
2. Ikada, Y.; Tsuji, H. Macromol Rapid Commun 2000, 21, 117.
3. Petersen, K.; Nielsen, P.; Olsen, M. Starch 2001, 53, 356.
4. Lunt, J. Polym Degrad Stab 1998, 59, 145.
5. Jacobsen, S.; Degee, P.; Fritz, H. G.; Dubois, P.; Jerome, R. Polym Eng Sci 1999, 39, 1311.
6. Auras, R.; Harte, B.; Selke, S. Macromol Biosci 2004, 4, 835.
7. Paul, M.-A.; Alexandre, M.; Degee, P.; Henrist, C.; Rulmont, A.; Dubois, P. Polymer 2003, 44, 443.
8. Chen, C.-C.; Chueh, J.-Y.; Tseng, H.; Huang, H.-M.; Lee, S.-Y. Biomaterials 2003, 24, 1167.
9. Yu, Z.; Yin, J.; Yan, S.; Xie, Y.; Ma, J.; Chen, X. Polymer 2007, 48, 6439.
10. Cabedo, L.; Feijoo, J. L.; Villanueva, M. P.; Lagaron, J. M.; Gimenez, E. Macromol Symp 2006, 233, 191.
11. Messersmith, P. B.; Giannelis, E. P. Chem Mater 1994, 6, 1719.
12. Yano, K.; Usuki, A.; Okada, A.; Kurauchi, T.; Kamigaito, O. J Polym Sci Part A: Polym Chem 1993, 31, 2493.
13. Usuki, A.; Kawasumi, M.; Kojima, Y.; Okada, A.; Kurauchi, T.; Kamigaito, O. J Mater Res 1993, 8, 1185.
14. Xu, R.; Manias, E.; Snyder, A. J.; Runt, J. Macromolecules 2001, 34, 337.
15. Ray, S. S.; Maiti, P.; Okamoto, M.; Yamada, K.; Ueda, K. Macromolecules 2002, 35, 3104.
16. Petersson, L.; Oksman, K.; Mathew, A. P. J Appl Polym Sci 2006, 102, 1852.
17. Wang, Y.; Chen, F.-B.; Li, Y.-C.; Wu, K.-C. Compos B 2004, 35, 111.
18. Wang, Y.; Chen, F. B.; Wu, K. C.; Wang, J. C. Polym Eng Sci 2006, 46, 289.
19. Ray, S. S.; Okamoto, M. Macromol Rapid Commun 2003, 24, 815.
20. Ray, S. S.; Yamada, K.; Okamoto, M.; Fujimoto, Y.; Ogami, A.; Ueda, K. Polymer 2003, 44, 6633.
21. Nam, P. H.; Kaneko, M.; Ninomiya, N.; Fujimori, A.; Masuko, T. Polym Int 2006, 55, 916.
22. Galgali, G.; Ramesh, C.; Lele, A. Macromolecules 2001, 34, 852.
23. Ren, G.; Silva, A. S.; Krishnammoorti, R. Macromolecules 2000, 33, 3739.
24. Li, J.; Zhou, C. X.; Wang, G.; Zhao, D. J Appl Polym Sci 2003, 89, 318.
25. Solomon, M. J.; Almusallam, A. S.; Seefeldt, K. F.; Varadan, P. Macromolecules 2001, 34, 1864.
26. Wu, D. F.; Zhou, C. X.; Xie, F.; Mao, D. L.; Zhang, B. Eur Polym J 2005, 41, 2199.
27. Wu, D. F.; Zhou, C. X.; Yu, W.; Xie, F. J Polym Sci Part B: Polym Phys 2005, 43, 2807.
28. Wu, D.; Wu, L.; Wu, L.; Zhang, M. Polym Degrad Stab 2006, 91, 1.
29. Bharadwaj, R. K. Macromolecules 2001, 34, 9189.
30. Drumright, R. E.; Gruber, P. R.; Henton, D. E. Adv Mater 2000, 12, 1841.
31. Cohn, D.; Hotovely Salomon, A. Biomaterials 2005, 26, 2297.
32. Aslan, S.; Calandrelli, L.; Laurenzio, P.; Malinconico, M.; Migliaresi, C. J Mater Sci 2000, 35, 1615.
33. Kim, C.-H.; Cho, K. Y.; Choi, E.-J.; Park, J.-K. J Appl Polym Sci 2000, 77, 226.
34. Shen, Y.; Sun, W.; Zhu, K. J.; Shen, Z. J Biomed Mater Res 2000, 50, 528.